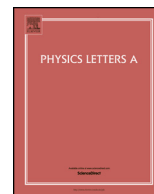




Contents lists available at ScienceDirect

Physics Letters A

www.elsevier.com/locate/pla



The bursts of high energy events observed by the telescope array surface detector

R.U. Abbasi^a, M. Abe^b, T. Abu-Zayyad^a, M. Allen^a, R. Anderson^a, R. Azuma^c, E. Barcikowski^a, J.W. Belz^a, D.R. Bergman^a, S.A. Blake^a, R. Cady^a, B.G. Cheon^e, J. Chiba^f, M. Chikawa^g, T. Fujiiⁱ, M. Fukushima^{i,j}, T. Goto^k, W. Hanlon^a, Y. Hayashi^k, N. Hayashida^l, K. Hibino^l, K. Honda^m, D. Ikedaⁱ, N. Inoue^b, T. Ishii^m, R. Ishimori^c, H. Itoⁿ, D. Ivanov^a, C.C.H. Jui^a, K. Kadota^o, F. Kakimoto^c, O. Kalashev^p, K. Kasahara^q, H. Kawai^r, S. Kawakami^k, S. Kawana^b, K. Kawataⁱ, E. Kidoⁱ, H.B. Kim^e, J.H. Kim^a, J.H. Kim^s, S. Kishigami^k, S. Kitamura^c, Y. Kitamura^c, V. Kuzmin^p, Y.J. Kwon^h, J. Lan^a, J.P. Lundquist^a, K. Machida^m, K. Martens^j, T. Matsuda^t, T. Matsuyama^k, J.N. Matthews^a, M. Minamino^k, K. Mukai^m, I. Myers^a, K. Nagasawa^b, S. Nagatakiⁿ, T. Nakamura^u, T. Nonakaⁱ, A. Nozato^g, S. Ogio^k, J. Ogura^c, M. Ohnishiⁱ, H. Ohokaⁱ, K. Okiⁱ, T. Okuda^{v,*}, M. Ono^w, R. Onogi^k, A. Oshima^x, S. Ozawa^q, I.H. Park^y, M.S. Pshirkov^{z,p}, D.C. Rodriguez^a, G. Rubtsov^p, D. Ryu^s, H. Sagawaⁱ, K. Saitoⁱ, Y. Saito^{ae}, N. Sakakiⁱ, N. Sakurai^k, A.L. Sampson^a, L.M. Scott^{aa}, K. Sekinoⁱ, P.D. Shah^a, F. Shibata^m, T. Shibataⁱ, H. Shimodairaⁱ, B.K. Shin^k, H.S. Shinⁱ, J.D. Smith^a, P. Sokolsky^a, R.W. Springer^a, B.T. Stokes^a, S.R. Stratton^{a,aa}, T.A. Stroman^a, T. Suzawa^b, M. Takamura^f, M. Takedaⁱ, R. Takeishiⁱ, A. Taketa^{ab}, M. Takitaⁱ, Y. Tameda^l, H. Tanaka^k, K. Tanaka^{ac}, M. Tanaka^t, S.B. Thomas^a, G.B. Thomson^a, P. Tinyakov^{p,ad}, I. Tkachev^p, H. Tokuno^c, T. Tomida^{ae}, S. Troitsky^p, Y. Tsunesada^k, K. Tsutsumi^c, Y. Uchihori^{af}, S. Udo^l, F. Urban^{ad}, G. Vasiloff^a, T. Wong^a, R. Yamane^k, H. Yamaoka^t, K. Yamazaki^{ab}, J. Yang^d, K. Yashiro^f, Y. Yoneda^k, S. Yoshida^r, H. Yoshii^{ag}, R. Zollinger^a, Z. Zundel^a

^a High Energy Astrophysics Institute and Department of Physics and Astronomy, University of Utah, Salt Lake City, UT, USA

^b The Graduate School of Science and Engineering, Saitama University, Saitama, Saitama, Japan

^c Graduate School of Science and Engineering, Tokyo Institute of Technology, Meguro, Tokyo, Japan

^d Department of Physics and Institute for the Early Universe, Ewha Womans University, Seodaemun-gu, Seoul, Republic of Korea

^e Department of Physics and The Research Institute of Natural Science, Hanyang University, Seongdong-gu, Seoul, Republic of Korea

^f Department of Physics, Tokyo University of Science, Noda, Chiba, Japan

^g Department of Physics, Kinki University, Higashi Osaka, Osaka, Japan

^h Department of Physics, Yonsei University, Seodaemun-gu, Seoul, Republic of Korea

ⁱ Institute for Cosmic Ray Research, University of Tokyo, Kashiwa, Chiba, Japan

^j Kavli Institute for the Physics and Mathematics of the Universe (WPI), Todai Institutes for Advanced Study, The University of Tokyo, Kashiwa, Chiba, Japan

^k Graduate School of Science, Osaka City University, Osaka, Osaka, Japan

^l Faculty of Engineering, Kanagawa University, Yokohama, Kanagawa, Japan

^m Interdisciplinary Graduate School of Medicine and Engineering, University of Yamanashi, Kofu, Yamanashi, Japan

ⁿ Astrophysical Big Bang Laboratory, RIKEN, Wako, Saitama, Japan

^o Department of Physics, Tokyo City University, Setagaya-ku, Tokyo, Japan

^p National Nuclear Research University, Moscow Engineering Physics Institute, Moscow, Russia

^q Advanced Research Institute for Science and Engineering, Waseda University, Shinjuku-ku, Tokyo, Japan

^r Department of Physics, Chiba University, Chiba, Chiba, Japan

^s Department of Physics, School of Natural Sciences, Ulsan National Institute of Science and Technology, UNIST-gil, Ulsan, Republic of Korea

^t Institute of Particle and Nuclear Studies, KEK, Tsukuba, Ibaraki, Japan

^u Faculty of Science, Kochi University, Kochi, Kochi, Japan

^v Department of Physical Sciences, Ritsumeikan University, Kusatsu, Shiga, Japan

^w Department of Physics, Kyushu University, Fukuoka, Fukuoka, Japan

* Corresponding author.

E-mail address: okuda@icrr.u-tokyo.ac.jp (T. Okuda).

^x Engineering Science Laboratory, Chubu University, Kasugai, Aichi, Japan^y Department of Physics, Sungkyunkwan University, Jang-an-gu, Suwon, Republic of Korea^z Sternberg Astronomical Institute, Moscow M.V. Lomonosov State University, Moscow, Russia^{aa} Department of Physics and Astronomy, Rutgers University – The State University of New Jersey, Piscataway, NJ, USA^{ab} Earthquake Research Institute, University of Tokyo, Bunkyo-ku, Tokyo, Japan^{ac} Graduate School of Information Sciences, Hiroshima City University, Hiroshima, Hiroshima, Japan^{ad} Service de Physique Théorique, Université Libre de Bruxelles, Brussels, Belgium^{ae} Department of Computer Science and Engineering, Shinshu University, Nagano, Nagano, Japan^{af} National Institute of Radiological Science, Chiba, Chiba, Japan^{ag} Department of Physics, Ehime University, Matsuyama, Ehime, Japan

ARTICLE INFO

Article history:

Received 12 January 2017

Received in revised form 12 June 2017

Accepted 13 June 2017

Available online xxx

Communicated by P.R. Holland

Keywords:

High energy radiation

Lightning

Terrestrial gamma-ray flash

ABSTRACT

The Telescope Array (TA) experiment is designed to detect air showers induced by ultra high energy cosmic rays. The TA ground Surface particle Detector (TASD) observed several short-time bursts of air shower like events. These bursts are not likely due to chance coincidence between single shower events. The expectation of chance coincidence is less than 10^{-4} for five-year's observation. We checked the correlation between these bursts of events and lightning data, and found evidence for correlations in timing and position. Some features of the burst events are similar to those of a normal cosmic ray air shower, and some are not. On this paper, we report the observed bursts of air shower like events and their correlation with lightning.

© 2017 Elsevier B.V. All rights reserved.

1. Introduction

There have been reports about the observation of energetic radiation from thunderclouds. Some of these reports discuss the increasing rates of radiation at the ground in the presence of thunderclouds. Some of them discuss bursts of energetic radiation observed from space, known as terrestrial gamma-ray flashes (TGF) [1,2], also from aircraft [3]. They are believed to be associated with upward lightning flashes at the tops of thunderclouds. The observation of TGF on the ground was reported by Dwyer, et al. [4] Other observations of energetic radiation have been associated with individual lightning processes in the flash. The possible mechanism for some of these kinds of energetic radiation from thunderclouds is Relativistic Runaway Electron Avalanches (RREAs) or due to strong electric field on the streamer tip summarized by Dwyer, et al. [5]

Lightning is classified by the discharge region, intracloud lightning (IC), cloud to ground lightning (CG) and cloud to cloud lightning. The natural lightning flash consists of several processes, known as the stepped leader, return stroke, dart leader and subsequent return stroke. The leader direction may be up or down and of positive or negative polarity, hence there are four types of lightning for cloud to ground lightning. However, except for lightning strikes on tall objects, most lightning starts with negative charges moving downward.

Moore, et al. [6] reported the observation of the energetic radiation from stepped leaders, using NaI as a radiation detector. Dwyer, et al. [7,8] reported the observation of the energetic radiation from dart leaders, also using NaI as a radiation detector, for rocket triggered lightning. Dwyer, et al. [9] reported the observation of energetic radiation from stepped leaders, and Dwyer, et al. [10] reported association with the return stroke, also using NaI as a radiation detector, for natural cloud to ground lightning.

On the other hand, the stepped leader, the beginning of lightning, cannot start only by the electric fields in the usual thunderstorm. Therefore, it has been hypothesized that cosmic ray air showers play a role in triggering lightning by ionizing the atmosphere. In support of this, there have been several reports of energetic radiation observed with lightning.

Gurevich, et al. [11,12] reported the coincidence of air showers with lightning, using NaI and gas-counters as radiation detectors. Chilingarian, et al. [13] also reported the coincidence of air show-

ers with lightning, using plastic scintillators. Gurevich, et al. [14] presented the results of radio emission measurements and discussed as follows. If cosmic ray air showers stimulate the electron avalanche in lightning, their observed radio event rates seem inconsistent with the flux of cosmic rays with energies estimated from the observed radio amplitudes of electron avalanche. The cosmic ray energies estimated from the avalanche amplitudes are five to six orders of magnitude higher than those estimated from the rates. Hydrometeors are introduced in an effort to overcome this inconsistency [14].

2. Observed burst events

The Telescope Array (TA) experiment, located in midwest Utah, USA(39.3N, 112.9W, Alt 1382 m), consists of two types of detector (Fig. 1). Both methods observe the high energy phenomenon known as an "air shower", which is generated by an ultra high energy cosmic ray. One instrument is atmospheric fluorescence telescope detectors and the other is ground surface particle detectors [15]. In contrast to atmospheric fluorescence which is observable during moonless nights, the TA Surface Detector (TASD) runs all day throughout the year. TASD consists of 507 plastic scintillation counters. The particle detecting part of an individual TASD counter is shown in Fig. 2. The energy deposition on this counter for a vertical muon is 2.043 MeV and the equivalent energy for trigger threshold is 0.7 MeV. The counters are deployed as a square grid array with 1.2 km spacing, and covers 680 km² altogether. When three adjacent detectors detect a signal, each of which corresponds to more than three particle equivalent in 8 μ s, TASD judges that their signals are from an air shower, causing signal waveforms to be digitized from all detectors within $\pm 32 \mu$ s of the trigger time [15]. The TASD is designed to detect all air showers from cosmic rays whose primary energy is more than 10^{19} eV. The average rate of shower trigger is 7.5 mHz and the expected cosmic ray energy at the threshold level is $10^{17.5}$ eV [15].

The particle detectors used in the preceding studies on introduction were mainly NaI, sometimes coupled with gas counters or plastic scintillators. The TASD uses plastic scintillator, with an area approximately 300 times larger than the NaI detectors but lacking the ability to measure the energy of individual particles. The TASD scintillator responds about 10 times faster than NaI. Whereas

Table 1

Reconstructed SD event list with NLDN lightning information. AS means air shower event observed by TASD, and LG means lightning event measured by NLDN. These X, Y, and zenith angle are relative to the TA site. The estimated AS zenith angle (in deg), LG peak current (in kA) are in same column. Alt parameter from shower front curvature and IC/CG flag for lightning are in the same column. The accuracy of zenith angle and alt parameter for these shower size are about 0.8(in deg) and about 100 m.

Event	Date yyyy/mm/dd	Time HH:MM:SS	μ sec [μ s]	X [km]	Y [km]	Zenith [deg] LG [kA]	Alt [km] IC/CG
AS	2010/10/04	16:58:42	930565	11.36	-7.43	15.7	4.0
AS	2010/10/04	16:58:42	930612	10.48	-7.37	13.1	4.4
AS	2010/10/04	16:58:42	930835	11.14	-8.16	27.7	3.3
LG	2010/10/04	16:58:42	930608	12.5	-5.1	-63.5	IC
LG	2010/10/04	16:58:42	934058	10.6	-8.1	-35.8	CG
AS	2011/07/27	08:06:15	124319	3.45	1.95	5.3	4.1
AS	2011/07/27	08:06:15	124543	2.90	2.23	19.2	3.1
LG	2011/07/27	08:06:15	124303	3.7	2.3	-35.6	IC
LG	2011/07/27	08:06:15	130887	3.1	2.0	-28.0	CG
AS	2011/09/16	19:40:56	567481	-3.21	-9.29	38.8	3.3
AS	2011/09/16	19:40:56	567566	-3.52	-9.41	32.2	3.1
AS	2012/07/06	01:49:11	184219	9.85	-10.70	24.2	3.8
AS	2012/07/06	01:49:11	184307	7.64	-9.67	23.6	3.4
LG	2012/07/06	01:49:11	184122	9.0	-9.7	-36.3	IC
AS	2012/09/07	01:55:45	380684	-8.64	1.25	14.9	4.5
AS	2012/09/07	01:55:45	380755	-9.86	-0.34	11.4	4.8
AS	2012/09/07	01:55:45	380881	-9.45	-0.96	31.7	3.4
LG	2012/09/07	01:55:45	380675	-9.0	0.7	-53.9	IC
LG	2012/09/07	01:55:45	390411	-9.6	-2.0	-20.1	CG
LG	2012/09/07	01:55:45	409370	-8.6	-1.7	-12.2	CG

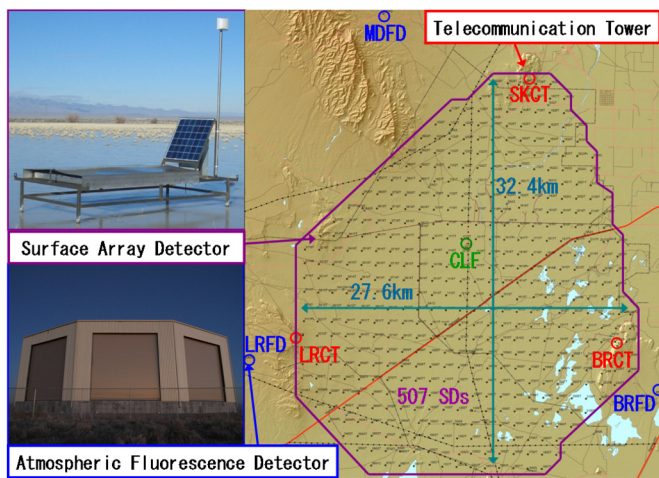


Fig. 1. Telescope Array Experiment. Totally 507 ground surface particle detectors (tiny dots above) are surrounded by three atmospheric fluorescence telescope stations (blue open circles). (For interpretation of the references to color in this figure legend, the reader is referred to the web version of this article.)

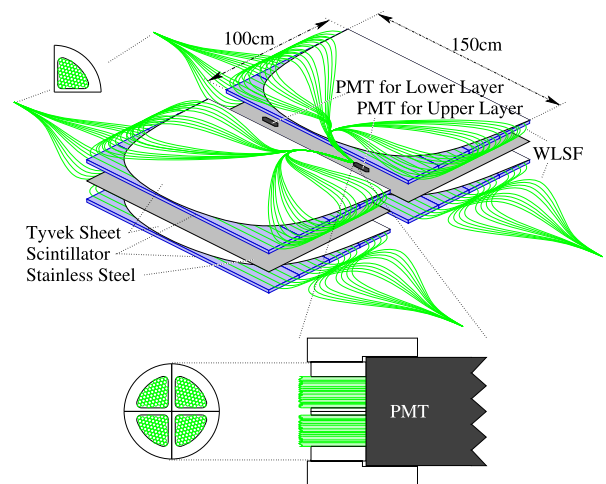


Fig. 2. Particle detecting part of TASD consists of two layers of plastic scintillator. Each scintillation layer has 1.2 cm thickness and is read out by wavelength-shifting fibers and one photomultiplier tube.

preceding detectors have been deployed over several square kilometers, the TASD covers about 300 times this area but is inefficient for small events due to the lower number density of the detectors.

In this paper we focus on TASD data collected from May 11, 2008 to May 04, 2013. We searched for temporal clusters of air shower events. We found ten cases in which at least three air shower triggers were recorded within 1 ms, called bursts. In each case, the air shower events within the burst are localized within a radius of approximately 1 km, although the position information was not a criteria of the search. Considering the events which could not generate shower triggers but were found in waveforms, the time gaps of events in a burst are distributed from several to a hundred microseconds. (See Fig. 11, for example.)

Five of the ten bursts contained events which were reconstructed, using a slightly modified air shower reconstruction program in which nonreconstructable preceding waveform units were removed from multi-waveform events. The reconstructed results are summarized in Table 1. Two views of burst events are shown in

Figs. 3 and 4 as examples. In the top panels of these three figures, the horizontal and vertical axes denote east/west and north/south coordinates in kilometers relative to the TA site, respectively. In addition, a typical (normal cosmic ray) air shower event view is shown in Fig. 5 for comparison. The zenith angle of the cosmic ray event is almost the same as that of the above two events, and its shower-size is between that of the two events. Fig. 6 shows the waveforms which compose each event.

The reconstructed air shower directions for individual bursts appear to point to small regions at altitudes lower than the expected first interaction depth of cosmic ray air showers of comparable size. All reconstructed air shower fronts for the burst events are much more curved than usual cosmic ray air showers. Please compare the middle plots in Figs. 3 and 4 for burst events and Fig. 5 for a normal event. In this reconstruction, the shower front is modeled as a sphere expanding at the speed of light from one point in the sky. Therefore, the altitude of this point, obtained from a fit, can be used as the parameter of shower front curvature. The altitude parameters of all reconstructed burst events are in a re-

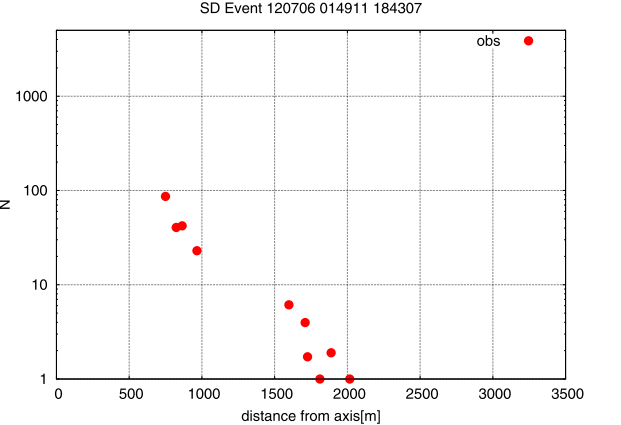
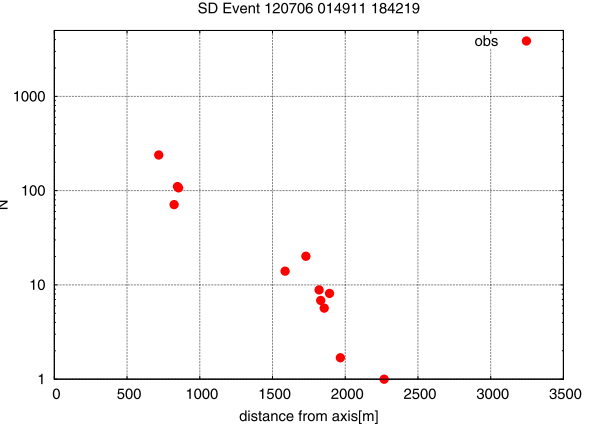
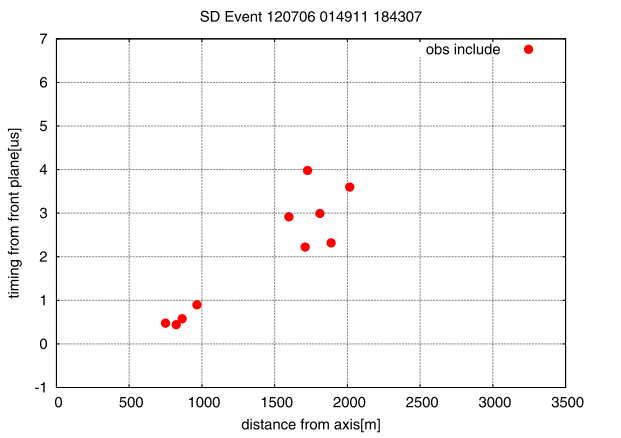
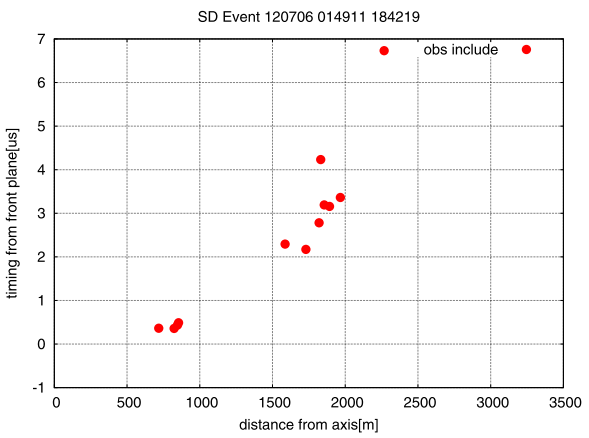
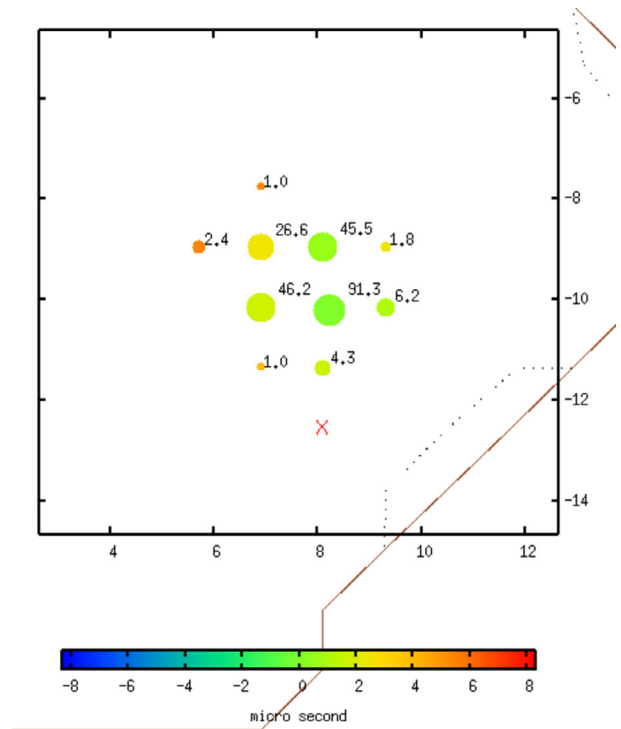
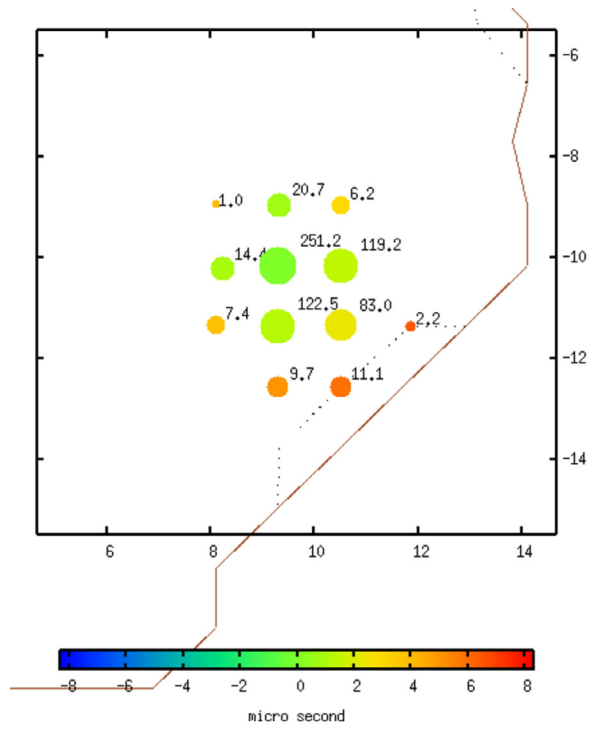


Fig. 3. Burst event 120706-014911-184219. Top: Particle hit mapping. The point size corresponds to the number of detected particles. The point color shows particle arrival timing. The adjacent number is vertical equivalent muon. Middle: Lateral arrival timing distribution. Bottom: Lateral distribution of the number of detected particles. (For interpretation of the references to color in this figure legend, the reader is referred to the web version of this article.)

Fig. 4. Burst event 120706-014911-184307. Top: Particle hit mapping. The point size corresponds to the number of detected particles. The point color shows particle arrival timing. The adjacent number is vertical equivalent muon. Middle: Lateral arrival timing distribution. Bottom: Lateral distribution of the number of detected particles. (For interpretation of the references to color in this figure legend, the reader is referred to the web version of this article.)

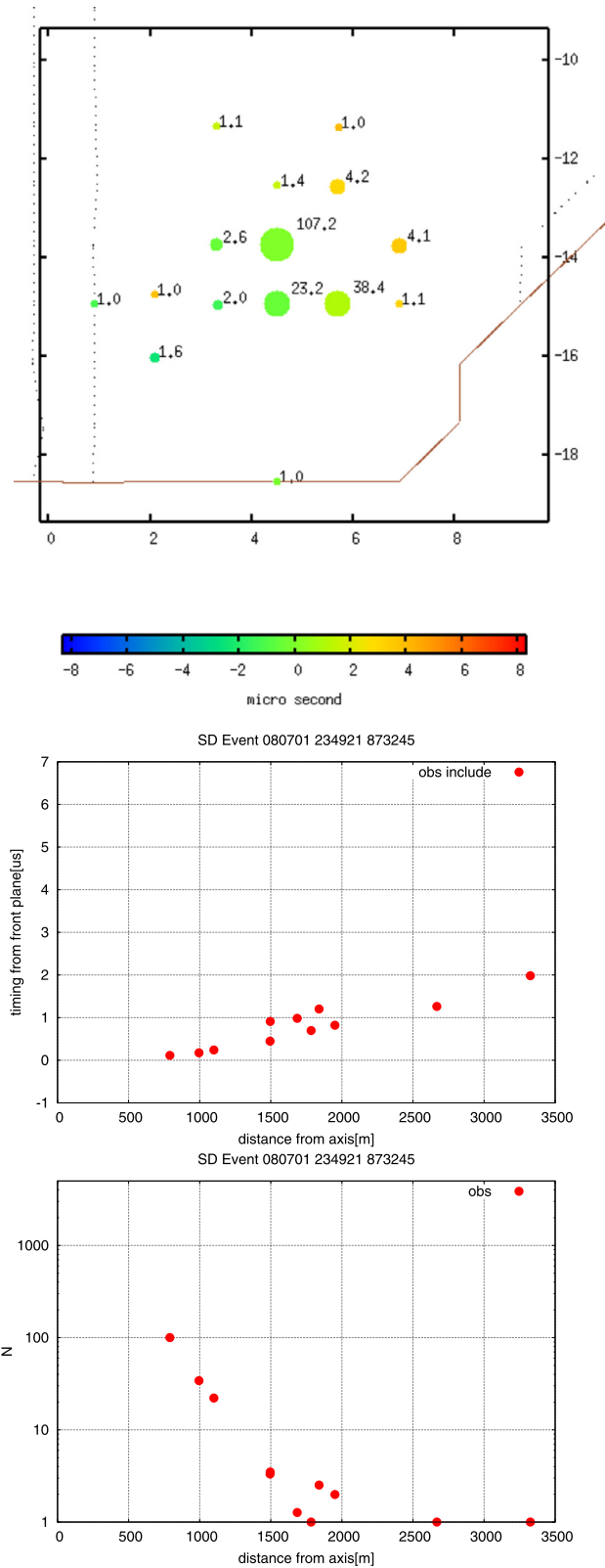


Fig. 5. Normal event 080701-234921-873245. Top: Particle hit mapping. The point size corresponds to the number of detected particles. The point color shows particle arrival timing. The adjacent number is vertical equivalent muon. Middle: Lateral arrival timing distribution. Bottom: Lateral distribution of the number of detected particles. (For interpretation of the references to color in this figure legend, the reader is referred to the web version of this article.)

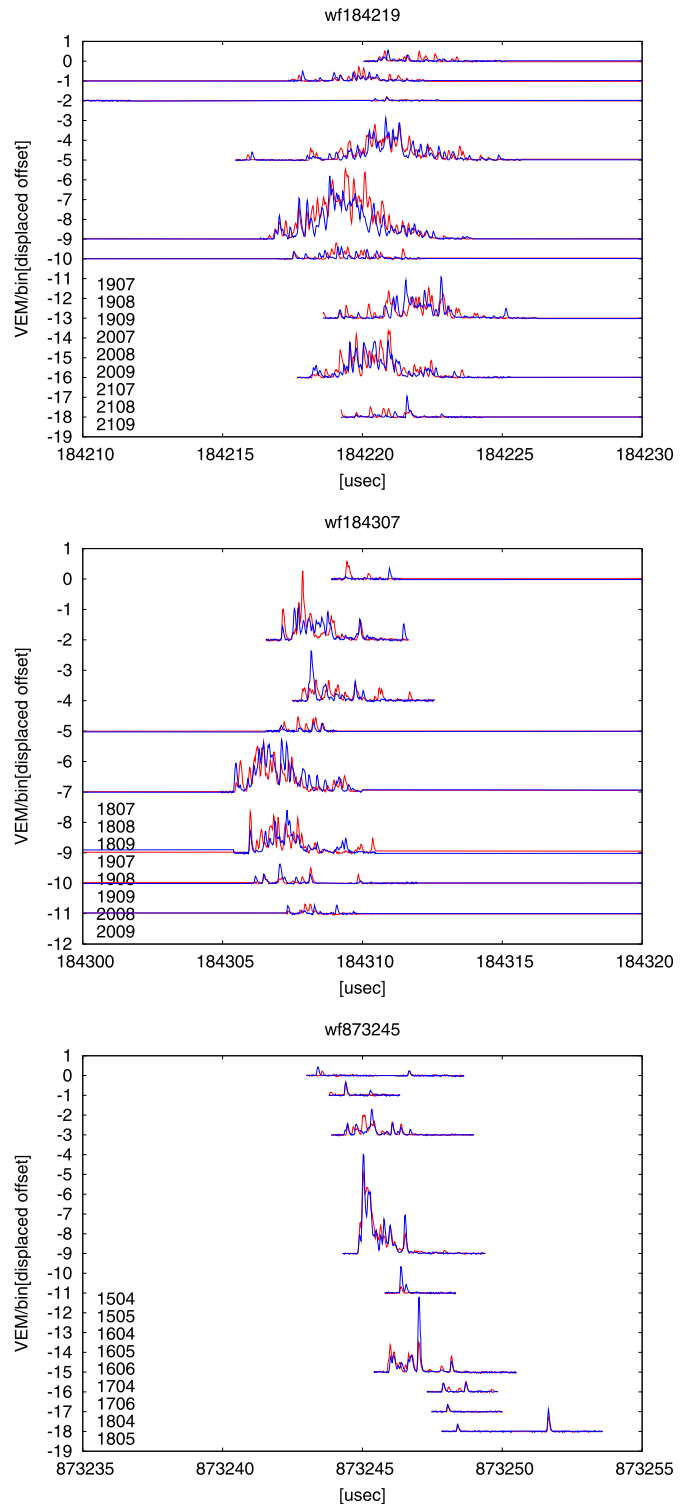


Fig. 6. Signal waveforms from SDs in the vicinity of shower core. Red and blue correspond to the two PMT channels for two layers of scintillator. Each horizontal level corresponds to the pedestal of individual SD. Vertical value has shifted to avoid superposition of waveforms from different SDs. Top: Burst event 120706-014911-184219. Middle: Burst event 120706-014911-184307. Bottom: Normal event 080701-234921-873245. (For interpretation of the references to color in this figure legend, the reader is referred to the web version of this article.)

gion much lower than that of usual cosmic ray air showers. This means that these burst showers seem to start developing at lower altitudes in the sky than normal air showers.

Waveforms of many burst events do not have sharp rising edges for SDs located near the shower core (Fig. 6). Burst event waveforms indicate that burst shower particles do not resemble normal cosmic ray air showers. However, time integrated energy deposit in the SDs is similar (please compare the bottom plots in Figs. 3 and 4 for burst events and Fig. 5 for a normal event), and can be fitted by a model from cosmic ray air shower simulation.

If these showers are induced by cosmic ray, the primary energy of cosmic ray is around 10^{18} to 10^{19} eV as estimated by signal amplitude and distribution. On the other hand, the event rate of 3 events in 1 ms in 1 km^2 is what is expected for a cosmic ray energy of about 10^{13} eV. Therefore, the estimated energy from individual events within the bursts is five to six orders of magnitude higher than the energy estimated by event rate. This inconsistency is quite similar to that discussed in Gurevich, et al. [14], which was mentioned in the introduction.

3. Correlation with lightning

We checked these bursts against the Vaisala lightning database. This database comes from U.S. National Lightning Detection Network (NLDN). NLDN detects lightning by multi-position very-low-frequency band antennas, and derives lightning information from radio arrival timing and waveform [16,17]. The database contains time, position, peak current and IC/CG flag. NLDN is somewhat inefficient for intracloud lightning detection [16]. The timing accuracy of lightning discharge is sub-microseconds [18].

NLDN lightning events were obtained which had a position within a 15 mile radius of the center of the TA site, and occurred between May 2008 and April 2013. The number of the detected lightning was 10073. 79% of the listed lightning events have flags indicating cloud to ground lightning. 85% of the listed lightning events have negative peak current. The location and peak current distributions of lightning on the list are shown in Fig. 7.

As summarized in Table 1, we searched for correlations in time between the five bursts of reconstructed events and lightning in the NLDN database. We categorize correlations into two types, “synchronized” and “related”.

The criteria by which lightning is characterized as synchronized is that the time difference between burst and lightning is less than 1 ms. Four bursts of the five are synchronized with lightning. Although there is no selection by position, all synchronized lightning is located in the vicinity of burst air shower events. All synchronized lightning events have flags that indicate intracloud lightning and negative peak current. By taking into account the intracloud lightning detection efficiency, the air shower bursts and lightning are well synchronized.

The search criteria for related lightning is that the time difference between burst and lightning is less than 200 ms, excepting synchronized lightning. Three bursts in the above four have related lightning in addition to synchronized lightning. Again, there is no selection by position but all related lightning is located in the vicinity of burst air shower events. All related lightning has a flag that indicates cloud to ground lightning, and negative peak current. These related lightning are subsequent lightning of synchronized lightning.

Our check of correlation between shower bursts and lightning shows that the observed shower bursts are clearly synchronized with negative intracloud lightning. The peak current of the synchronized lightning is very large for the currents observed for negative intracloud lightning (see the bottom of Fig. 7 and Table 1). Therefore, these bursts are very rare phenomena.

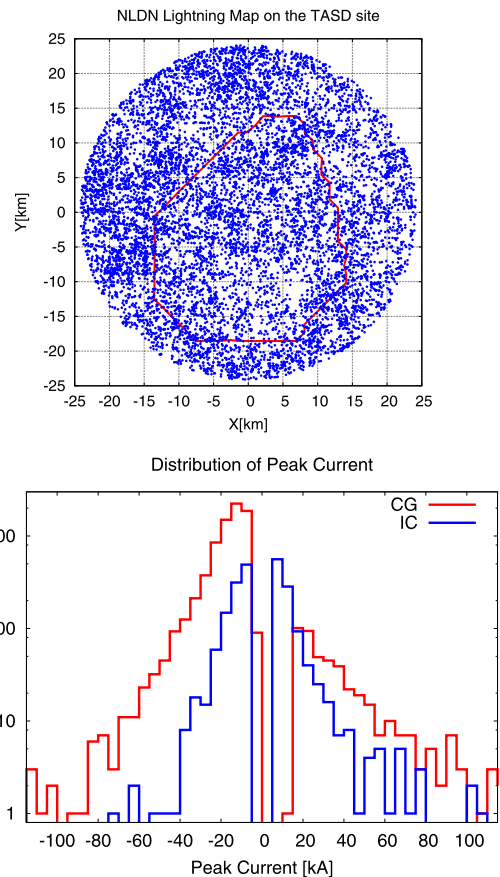


Fig. 7. NLDN data distributions. Top: Lightning map on the TA site. Blue points show individual strokes. The red line shows the outline of the TASD. Bottom: Peak current distributions for intracloud lightning in blue and cloud to ground lightning in red. (For interpretation of the references to color in this figure legend, the reader is referred to the web version of this article.)

The other five bursts which do not have reconstructed events. There is one burst which has synchronized and related lightning. There is another burst which has only related lightning. There are three bursts which do not have synchronized or related lightning. In addition, it was confirmed all of ten bursts are under thunderstorm.

A geometrical example of a reconstructed burst event with correlated lightning is shown in Fig. 8. The individual reconstructed events of this burst are shown in Fig. 3, 4 and the top two panels of Fig. 6. The lightning position is shown by a blue circle with radius which is approximately the typical position error [18]. The two reconstructed showers appear to come from nearby vertices at altitudes lower than the expected first interaction depth of cosmic ray air showers of comparable size.

We also considered correlations between lightning and all SD events, regardless of whether the SD events are part of a burst. The time difference between all SD events and lightning is shown in Fig. 9. The positive side of Fig. 9 indicates that the SD events occur nearly at the same time of lightning or earlier than lightning. Therefore, SD events correlated with lightning are associated with the initial processes of the lightning flash.

The breakdown of the correlation of all events is provided here. There are some chance correlations which can be easily identified by spatial localization. There are some two-event bursts, although the definition of burst in this paper is three or more events in 1 ms. There are many single correlated events. For the correlated lightning, their properties are similar to those which are correlated to the bursts described above. Synchronized lightning appears to

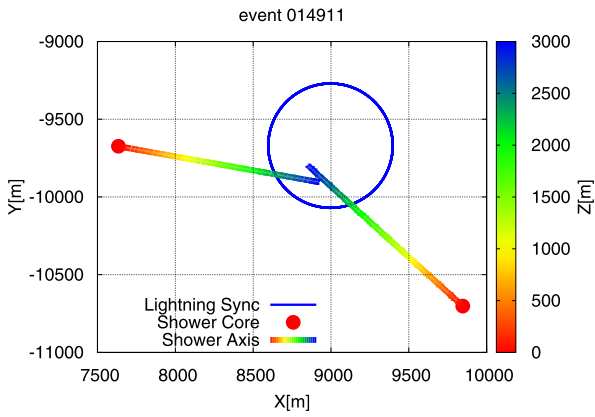


Fig. 8. The color scale shows the height from ground up to 3,000 m. The red points show shower core hit positions. The blue circle shows lightning position with 300 m radius of uncertainty. Synchronized (intracloud) lightning is set at $z = 3,000$ m. (For interpretation of the references to color in this figure legend, the reader is referred to the web version of this article.)

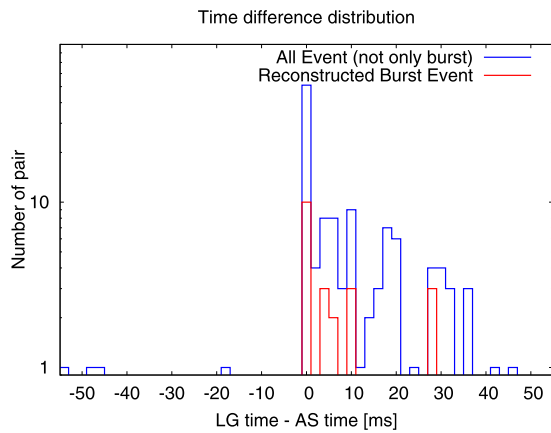


Fig. 9. Time difference between lighting and all TASD events (including non-burst events). The bin width is 2 ms. Synchronized lightning occurs in the central bin. The remainder of bins are included in the category of related lightning.

have the flag indicating intracloud lightning, and negative peak current. Related lightning tends to have the flag indicating cloud to ground lightning, and negative peak current.

4. Comparison with precedents

The TASD burst events have similar features to prior observations.

Dwyer, et al. [9] reported high energy radiation on the ground from each step of the stepped leader process. The time intervals of the stepped leader are in the 10 microsecond to 100 microsecond range. TASD burst events have time intervals of similar duration.

Several satellites observed high energy radiation bursts correlated with lightning. Cummer, et al. [19] reported high energy radiation detected by satellite, which is correlated with positive lightning. In contrast, TASD burst events on the ground are correlated with negative lightning. In both situations, the electric field direction works to accelerate electrons towards the detector.

Briggs, et al. [2] reported high energy radiation at satellite, which shows roughly two types of burst waveforms. One is Gaussian like and the other is log-normal like. TASD burst events also have roughly two type of waveforms. Fig. 10 is Gaussian like, and Fig. 11 is log-normal like. Although the signal shapes of TASD burst events and terrestrial gamma-ray flashes detected by satellite are similar, the signal timescale of SD events is about 2 orders of magnitude shorter. This can be due to the difference of the size of

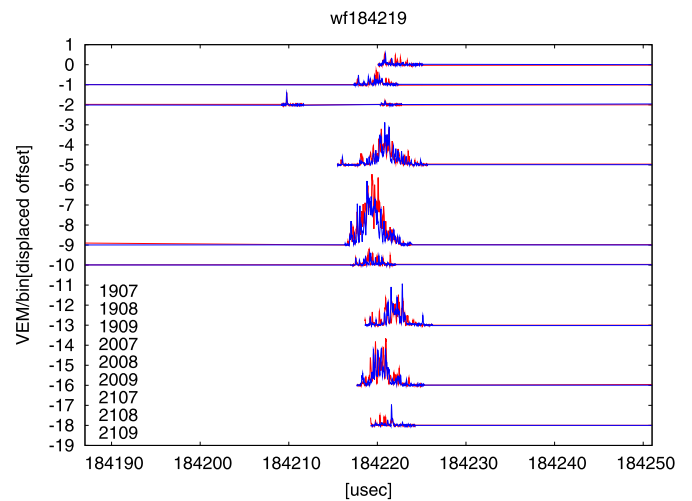
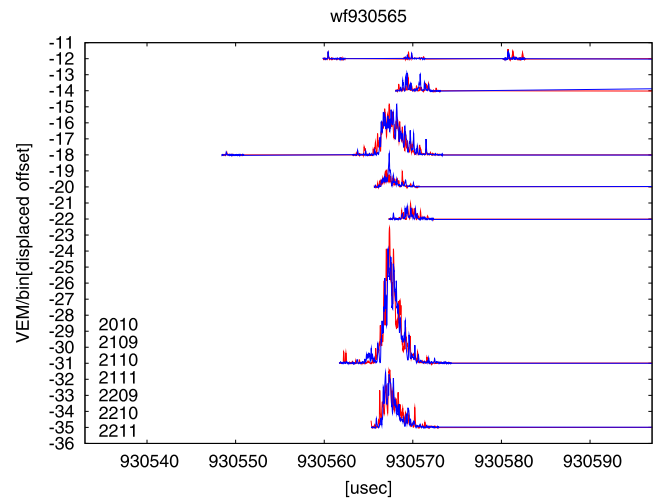


Fig. 10. Gaussian like waveforms from SDs in the vicinity of the shower core. Red and blue correspond to two PMT channels for two layers of scintillator. Each horizontal level corresponds to the pedestal of individual SD. Vertical value has been shifted to avoid superposition of waveforms from different SDs. (For interpretation of the references to color in this figure legend, the reader is referred to the web version of this article.)

accelerating region or the distance between the radiating point and the detector.

5. Conclusion and discussion

We have detected bursts of high energy events using the TASD. By comparing the times and positions of these events with lightning data in the NLDN database, we infer that these events seem to come from negative high current intracloud lightning. There is no evidence that burst events come from cloud to ground lightning.

What generates these individual events in a burst? We do not have a clear answer. The event rates in bursts are inconsistent with the flux of cosmic rays with energies estimated by deposited energies in SDs. By the time interval of events in a burst, it seems that they come from the stepped leader process. We summarize the features of the TASD bursts:

1. This burst phenomenon does not come from thunderstorm intermittently. It comes from negative high current intracloud lightning.
2. The reconstructed shower directions, within reconstruction accuracy, indicate that they come from a small region at low altitudes in the sky.

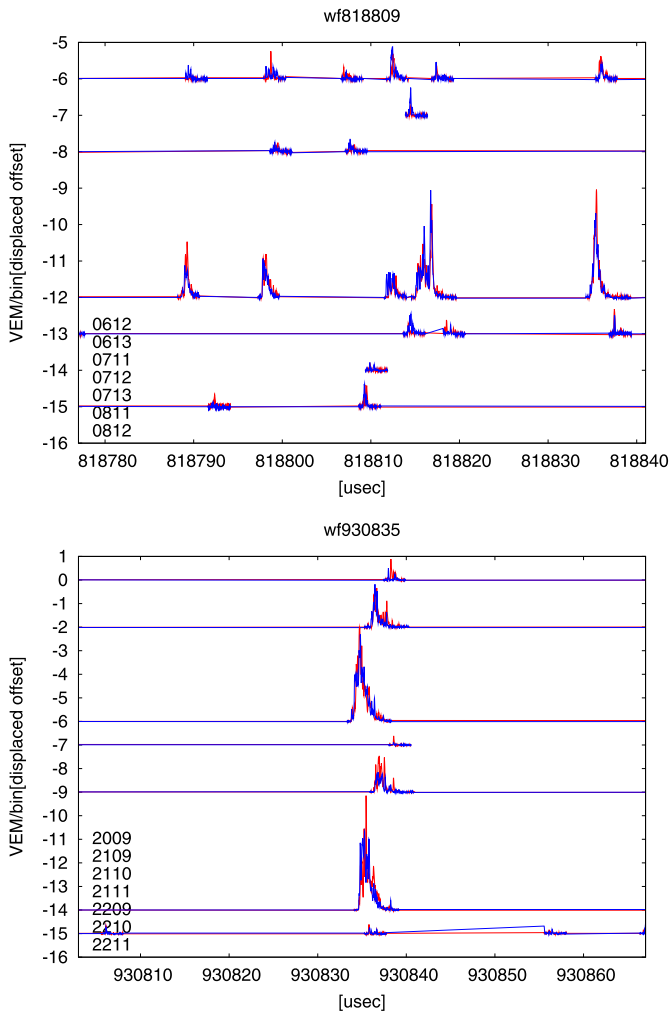


Fig. 11. Log-normal like waveforms from SDs in the vicinity of the shower core. Red and blue correspond to two PMT channels for two layers of scintillator. Each horizontal level corresponds to the pedestal of individual SD. Vertical value has been shifted to avoid superposition of waveforms from different SDs. (For interpretation of the references to color in this figure legend, the reader is referred to the web version of this article.)

3. These showers seem to start development at low altitudes in the sky, as determined by shower front curvature.
4. The time gap of detected radiation on the waveform is consistent with stepped leader process. (Several tens of microseconds.) These showers are generated at the initial processes of the lightning flash.
5. There is a less-sharp rising edge feature on the waveform at the detectors near shower cores for many burst events, as compared to cosmic ray air showers.

To prior observations of energetic radiation associated with lightning, we add somewhat unique information. The TASD is a significantly larger detector which uses fast scintillator waveforms,

allowing the reconstruction of spatial information for high energy radiation associated with negative high-current intracloud lightning.

Acknowledgements

The Telescope Array experiment is supported by the Japan Society for the Promotion of Science through Grants-in-Aid for Scientific Research on Specially Promoted Research (21000002) “Extreme Phenomena in the Universe Explored by Highest Energy Cosmic Rays” and for Scientific Research (19104006), and the Inter-University Research Program of the Institute for Cosmic Ray Research; by the U.S. National Science Foundation awards PHY-0307098, PHY-0601915, PHY-0649681, PHY-0703893, PHY-0758342, PHY-0848320, PHY-1069280, PHY-1069286, PHY-1404495 and PHY-1404502; by the National Research Foundation of Korea (2007-0093860, 2012R1A1A2008381, 2013004883); by the Russian Academy of Sciences, RFBR grant 11-02-01528a and 13-02-01311a (INR), IISN project No. 4.4502.13; and Belgian Science Policy under IUAP VII/37 (ULB). The foundations of Dr. Ezekiel R. and Edna Wattis Dumke, Willard L. Eccles and the George S. and Dolores Dore Eccles all helped with generous donations. The State of Utah supported the project through its Economic Development Board, and the University of Utah through the Office of the Vice President for Research. The experimental site became available through the cooperation of the Utah School and Institutional Trust Lands Administration (SITLA), U.S. Bureau of Land Management, and the U.S. Air Force. We also wish to thank the people and the officials of Millard County, Utah for their steadfast and warm support. We gratefully acknowledge the contributions from the technical staffs of our home institutions. An allocation of computer time from the Center for High Performance Computing at the University of Utah is gratefully acknowledged.

The lightning data used in this paper was obtained from Vaisala, Inc. We appreciate Vaisala’s academic research policy. And we appreciate the Mitsubishi Foundation to finalize this paper.

References

- [1] G.J. Fishman, et al., *Science* 264 (1994) 1313–1316.
- [2] M.S. Briggs, et al., *J. Geophys. Res.* 115 (2010) A07323.
- [3] D.M. Smith, et al., *J. Geophys. Res.* 116 (2011) D20124.
- [4] J.R. Dwyer, et al., *Geophys. Res. Lett.* 31 (2004) L05119.
- [5] J.R. Dwyer, et al., *Space Sci. Rev.* 173 (2012) 133–196.
- [6] C.B. Moore, et al., *Geophys. Res. Lett.* 28 (2001) 2141–2144.
- [7] J.R. Dwyer, et al., *Science* 299 (2003) 694–697.
- [8] J.R. Dwyer, et al., *Geophys. Res. Lett.* 31 (2004) L05118.
- [9] J.R. Dwyer, et al., *Geophys. Res. Lett.* 32 (2005) L01803.
- [10] J.R. Dwyer, et al., *J. Geophys. Res.* 117 (2012) A10303.
- [11] A.V. Gurevich, et al., *Phys. Lett. A* 373 (2009) 3550–3553.
- [12] A.V. Gurevich, et al., *J. Phys. Conf. Ser.* 409 (2013) 012234.
- [13] A. Chilingarian, et al., *Phys. Rev. D* 83 (2011) 062001.
- [14] A.V. Gurevich, A.N. Karashtin, *Phys. Rev. Lett.* 110 (2013) 185005.
- [15] T. AbuZayyad, et al., *NIM Phys. Res. A* 689 (2012) 87–97.
- [16] K.L. Cummins, M.J. Murphy, *IEEE Trans.* 51 (3) (2009) 499–518.
- [17] A. Nag, et al., *J. Geophys. Res.* 116 (2011) D02123.
- [18] K.L. Cummins, et al., in: *Proc. ILDC2010*, 2010.
- [19] S.A. Cummer, et al., *Geophys. Res. Lett.* 32 (2005) L08811.